Article

Epitaxial Growth of Quinacridone Derivative on Ag(110) Studied by Scanning Tunneling Microscopy

X. B. He, J. M. Cai, D. X. Shi, Y. Wang, and H.-J. Gao

J. Phys. Chem. C, **2008**, 112 (18), 7138-7144 • DOI: 10.1021/jp0767359

Epitaxial Growth of Quinacridone Derivative on Ag(110) Studied by Scanning Tunneling Microscopy

X. B. He,[†] J. M. Cai,[†] D. X. Shi,[†] Y. Wang,[‡] and H.-J. Gao*,[†]

Beijing National Laboratory of Condensed Matter Physics, Institute of Physics, Chinese Academy of Sciences, P.O. Box 603, Beijing 100190, China, and Key Lab of Supramolecular Structure and Materials, College of Chemistry, Jilin University, Changchun 130023, China

Received: August 22, 2007; In Final Form: February 8, 2008

The growth behavior of a layer of a quinacridone derivative (QA16C) on the Ag(110) surface was studied using low-temperature scanning tunneling microscopy. At very low coverage, molecule−substrate interactions determine the adsorption sites of QA16C molecules on Ag(110), and two distinct orientations of single molecules can be observed on silver terraces. At higher coverages up to 1 ML, intermolecular interactions drive the QA16C molecules to form rowlike nanostructures. Meanwhile, step-edge alignments of silver substrate induced by adsorbed organic molecules can be observed at very low coverage and at monolayer coverage. When the QA16C molecule coverage increases further to the second layer, different rowlike structures are formed. Intermolecular interactions, such as hydrogen bonds and alkyl−alkyl and $\pi-\pi$ interactions, dominate the second-layer structure. In addition, we show that the second layer of QA16C molecules can be controlled by increasing the growth temperature during deposition.

1. Introduction

The potential of using organic semiconductors as active materials in devices such as low-voltage-powered organic light-emitting devices (OLEDs), organic field-effect transistors (OFETs), and molecular electronic devices has attracted great interest in both basic scientific research and technological applications.[1−6] To optimize device performance, the details of the interfacial structure have to be controlled carefully during the aggregation, packing, and orientation processes of the growth especially on different substrates such as metals, semiconductors, glass, and polymers, which are important for charge injection, transport, and light emission characteristics. Much effort has recently been made to understand and develop self-assembled systems that provide a facile bottom-up approach for the construction of molecule-scale nanostructures by adjusting the subtle balance between the competition of molecule−substrate and intermolecular interactions.[7]

Among many important organic semiconductor materials, quinacridone (QA) and its derivatives are well-known organic pigments and dopant emitters that display excellent chemical stability,[8−11] as well as very pronounced photovoltaic and photoconductive activities. Because of their good electrochemical stability in solids and light photoluminescence in dilute solutions, quinacridone and its derivatives are promising materials for the fabrication of high-performance organic light-emitting devices.[12−14] Moreover, many investigations on quinacridone derivatives have been performed to explore the assembly and structural properties of the solid−liquid interface. For example, the De Feyter group applied scanning tunneling microscopy (STM) to study the aggregation behavior and two-dimensional (2D) order of 2,3,9,10-tetra(dodecyloxy)quinacridone, 2,9-di-(2-undecyltridecyl-1-oxy)quinacridone, and *N*,*N*′-dimethyl-substituted analogues on highly oriented pyrolytic graphite (HOPG).[15,16] Zhang et al. reported 2D self-assemblies of a series of *N*,*N*′-dialkyl-substituted quinacridone derivatives on the HOPG−solution interface. They found that this system can be fine-tuned by coadsorbing the QA derivatives with monofunctional acid or bifunctional dicarboxylic acids[17−19] and that it can also form chiral racemates in the coadsorbed structures.[18]

In a solution environment, it is difficult to follow the initial stage and second-layer structure of quinacridone derivatives, because of the presence of the surrounding solution. Organic molecular beam epitaxy (OMBE) is widely used to grow ordered organic films on crystalline surfaces and allows the study of epitaxial growth from low coverage to coverage of several layers.[20] Although several studies have been reported on the growth of monolayers of quinacridone derivatives,[21,22] to the best of our knowledge, a systematic study on the growth from submonolayer to multilayer coverage has not been reported. The ultrahigh-vacuum (UHV) OMBE technique provides a better environment than the liquid−solid interface for studying the growth process and understanding the subtle interactions involved. In a previous work, we reported that self-assemblies of quinacridone derivatives can be modulated by lateral alkyl chains on the Ag(110) surface in UHV.[22] The QA molecular structure can be modified by substituting C atoms with N and O and by attaching lateral alkyl chains to the N atoms. Figure 1e shows the molecular structure of a quinacridone derivative denoted as QA16C.

In this article, we present a study of the growth of a layer of QA16C molecules adsorbed on the Ag(110) surface in UHV in the range from low submonolayer to monolayer coverage and the structure of the second layer using low-temperature scanning tunneling microscopy (LT-STM). We systematically investigated the specific adsorption sites at the initial stage as well as the ongoing self-assembled structure. The results are helpful in understanding the interactions between the organic molecules and the noble metal substrate. In addition, this UHV work is

* Corresponding author. E-mail: hjgao@aphy.iphy.ac.cn.
[†] Chinese Academy of Sciences.
[‡] Jilin University.

10.1021/jp0767359 CCC: $40.75
Published on Web 04/16/2008

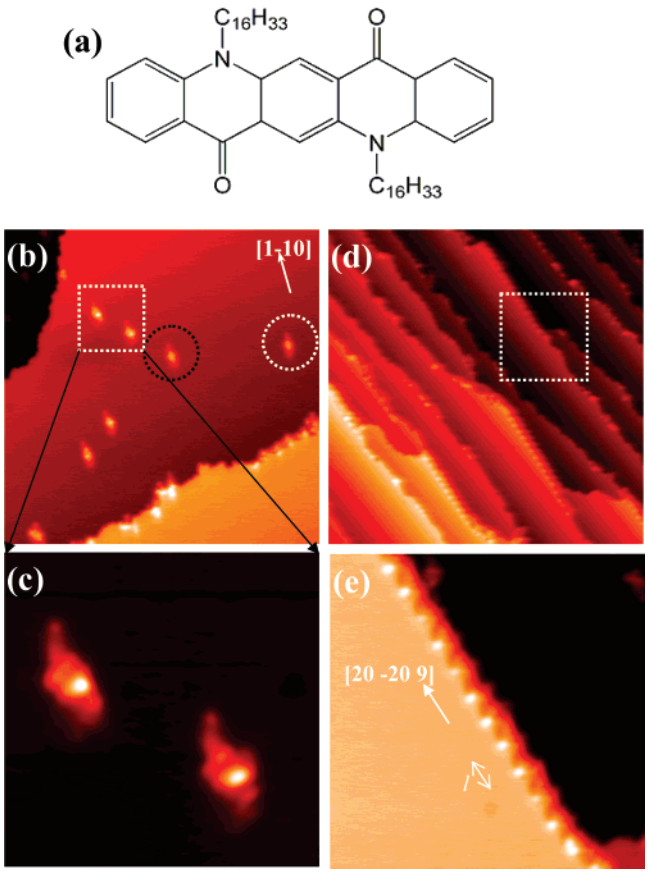

Figure 1. (a) Schematic of the molecular structure of quinacridone derivative QA16C. At very low coverage, the molecular orientations adsorbed (b) on large open silver terraces and(d) at step edges are quite different. (b) On large open silver terraces, exactly two distinct molecular orientations, indicated by black and white circles, exist, implying strong substrate−molecule interactions. The Ag[1−10] direction is also indicated by the white arrow. Conditions: area = 70 nm × 70 nm, $V_{sample} = -1.2$ V, $I = 0.05$ nA. (c) High-resolution STM image for single QA16C on silver terrace. Conditions: area = 15 nm × 15 nm, $V_{sample} = -1.2$ V, $I = 0.05$ nA. (d) QA16C molecules adsorbed at the step edge of Ag(110). Most of these molecules are observed to align regularly with lengths of up to several tens of nanometers along the Ag[20 −20 9] direction. This molecular alignment can be observed only at step edges with heights of two atomic layers, whereas a few molecules are adsorbed at step edges of a single atomic terrace, as shown in the dashed rectangle. Conditions: area = 120 nm × 120 nm, $V_{sample} = -0.8$ V, $I = 0.2$ nA. (e) High-resolution STM image of QA16C molecules at a silver step edge. Conditions: area = 30 nm × 30 nm, $V_{sample} = -0.8$ V, $I = 0.2$ nA.

beneficial in establishing a technique for developing a better understanding of more complex self-assembly processes at the liquid−solid interface, where the presence of solvent leads to modified interaction forces.[23]

2. Experimental Details

All experiments were performed in a combined UHV system equipped with OMBE and Omicron LT-STM instruments. The base pressure was 1×10^{-10} Torr. The single-crystal Ag(110) substrate (99.999% and orientation accuracy <0.1°) was purchased from MaTeck GmbH (Juelich, Germany). Before being placed under UHV conditions, the Ag(110) substrate was mechanically polished. A clean Ag(110) surface was obtained by at least three cycles of sputtering and annealing (sputtering at 5×10^{-6} Torr Ar pressure with an ion energy of 1 keV and a surface ion flux of 5.9 μA/cm^2 for 20 min; annealing at about 700 K for 20 min). Then, the cleanliness of the surface was checked by low-energy electron diffraction (LEED) and LT-STM. The QA16C material was purified using the established methods[10] by several cycles of temperature-gradient sublimation in vacuum and was then immediately loaded into a sublimation cell. The cell was kept at 400 K for several hours to be degassed thoroughly before evaporation experiments. The deposition rate of QA16C was about 0.4 ML min^{-1} at the evaporation temperature of 488 K. The deposition rate can be monitored and controlled precisely by in situ LEED observation. Here, we define a monolayer (ML) as a molecular coverage of about 3.7×10^{13} molecules per cm^2, referred to the most relevant monolayer packing (see Figure 3 below). The temperature of silver substrate was maintained at room temperature and above during the deposition. Then, the samples were transferred to the STM chamber for STM measurements. All of the STM images in this article were recorded in constant-current mode at 78 K. Chemically etched tungsten tips were used for the STM experiments, and in our STM measurements, the voltage bias refers to the sample voltage with respect to the tip.

3. Results and Discussion

The first measurements were made on a submonolayer coverage of QA16C on Ag(110). Subsequently, the coverage was increased slowly to 1.7 ML. For better clarity, we subdivide this section into three subsections in which we address the QA16C structure first in the submonolayer regime, then in the completed monolayer regime, and finally in the regime of rowlike structures formed in the second layer.

3.1. Submonolayer Regime. *Low Coverage.* QA16C molecules were deposited onto the Ag(110) substrate at room temperature. It is difficult to image QA16C on Ag(110) at room temperature at low molecular coverage. We attribute this difficulty to the high mobility of the molecules on the Ag(110) surface at ambient temperature. Then, we cooled the samples to 78 K at a low cooling rate. From the fast diffusion at ambient temperature and the low cooling rate, we assume that all of the molecular arrangements observed at 78 K represent thermodynamically stable structures. At very low coverages up to 0.1 ML, the molecules absorb on both large open silver terraces and at the step edges but with different orientations. As shown in Figure 1b, isolated molecules are randomly distributed on large open silver terraces, and exactly two distinct molecular orientations exist that allow the accommodation of the molecular units at sites on the anisotropic substrate with high symmetry. Submolecular resolution was achieved as shown in Figure 1c, in which the alkyl chains of QA16C can clearly be observed. The two molecular orientations on the silver terraces imply that the interactions between organic molecule and silver substrate are strong enough to determine the QA16C adsorption sites.[22]

A single molecule adsorbed on a step edge is different from the situation on large open terraces, as shown in Figure 1d. Most of these molecules are aligned in order, and the length is up to several tens of nanometers along specific silver step edges. All of these silver step edges are in the Ag[20 −20 9] direction. Figure 1e shows the details of the molecular alignment at the silver step edges. The distance between QA16C molecules, marked as l, is uniform at 2.9 ± 0.1 nm. Every molecule in Figure 1e behaves as a small protrusion about 0.05 nm in height with respect to the upper silver terrace. These molecular protrusions are quite a bit smaller than QA16C on the silver terrace, with an average height of 0.11 ± 0.01 nm. We propose that the molecules adsorbed on the step edges are in a different orientation of lying at the corner because adsorbate species usually interact more strongly with the substrate atoms on a

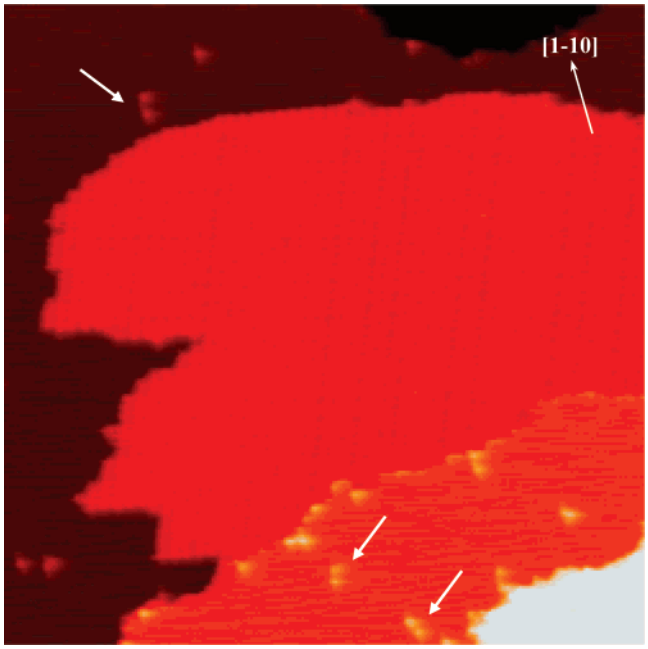

Figure 2. Typical STM image of about 0.4 ML of QA16C molecules on the Ag(110) surface. QA16C molecules prefer to aggregate to form molecular islands on large silver terraces rather than to form individual ones. Conditions: area = 150 nm × 150 nm, $V_{sample} = -0.8$ V, $I = 0.2$ nA.

transition metal surface at the kinks and step edges than on flat terraces. It should be pointed out that this ordered molecular alignment occurs only at step edges with a height of two silver atoms, whereas few molecules are adsorbed on step edges with heights of a single atom, as shown in the dashed rectangle in Figure 1d. We attribute this phenomenon to the lack of room for the QA16C molecule to reside at step edges with single-atom height.

In general, the step edges of a clean Ag(110) substrate are mostly along the Ag[1−10] and Ag[001] directions and extend like an irregular sawtooth for tens of nanometers, as shown in our previous STM experiments.[24] One possible reason for the molecular alignment along the Ag[20 −20 9] direction at low QA16C coverage is that the adsorbed QA16C molecules drive the silver atoms at the step edges to align in this specific direction to achieve the most stable configuration. In the following section, we show that this explanation is justified.

High Coverage. Figure 2 displays a typical STM image of about 0.4 ML of QA16C molecules on the Ag(110) surface. At this coverage, it is interesting to see that most of the QA16C molecules prefer to aggregate to form molecular islands on large silver terraces. This fact implies that the intermolecule interactions play an important role during the growth process. The molecular island always grows from the inner step edge to extend to the outer step edge on the terrace. The molecules in islands are highly regular in forming a rowlike structure. Considering that the conjugated parts of the molecules always show a higher tunneling probability than the alkyl parts, the bright protrusions in the STM image are attributed to the backbone of QA16C, whereas the dark stripes are assigned to the alkyl chains.[25] In addition, several dispersed QA16C molecules can be observed nearby, and some dimer-like molecular structures, pointed out by white arrows in Figure 2, can also be observed.

3.2. Monolayer Regime. After a saturated QA16C monolayer was deposited on Ag(110) at room temperature, as shown in Figure 3a, a large area of ordered rowlike nanopatterns was achieved. The uniform QA16C rowlike structures, extending along the [5−53] direction toward the Ag(110) step edge, can reach several hundred nanometers depending on the width of the terraces on the Ag(110) surface. The distance between neighboring rows is 2.91 ± 0.05 nm. Normally, only one symmetrical domain exists even on a large silver terrace, and the domain covers the terrace compactly with few defects, as shown in Figure 3a. In Figure 3b, we show an infrequent boundary of two symmetrical QA16C domains on the same terrace. This boundary is irregular and contains some holes because of the mismatch between these two structures. The mismatch increases the surface energy as molecules are adsorbed on the silver substrate.

Figure 3c presents the details of the monolayer rowlike structure. The QA16C molecules are displayed in this high-resolution STM image using a ball-and-stick model. We clearly see that the QA16C molecules are organized into rows along the [5−53] direction and are separated by the alkyl chains, which are interdigitated over their full length and aligned with their long axis parallel to the substrate surface. At the liquid−HOPG interface, structures with interdigitated alkyl chains are often observed with the alkyl chains oriented parallel to the ⟨1100⟩ directions of the HOPG substrate.[26−28] This is because of the fortuitous match of the distance between the centers of the hexagons of the graphite lattice, 2.46 Å, and the distance between alternate methylene groups of the alkyl chains, 2.51 Å.[29] However, there are few reports about this behavior for a metal−UHV interface with no C═C−C substrate along the alkyl chain direction. The angle between the QA16C backbone and the Ag[1−10] direction is 21 ± 2°. The alkyl chains are almost parallel to each other at an angle of 108° ± 2° with respect to the backbone of QA16C molecule. A high-resolution STM image of the alkyl chains, as shown in Figure 3d, reveals further structural details along the interdigitated alkyl chains. The zigzag-shaped row of spots for every alkyl chain is visible, and the distance between alternate spots in the rows, about 0.26 ± 0.01 nm, is consistent with the calculated value of 0.251 nm for alkyl chains.[28] This result suggests that the plane of the alkyl chains lies parallel to the substrate, as we show in the following model.

The Fourier transforms of many images of the molecular adlayer in this configuration provide mean values of the unit cell parameters, which are $a = 1.07 \pm 0.03$ nm and $b = 2.95 \pm 0.03$ nm, with a rotation angle of 103 ± 2°, as shown in Figure 3c. We propose the following matrix to describe the commensurate superstructure of QA16C on Ag(110)

$$\text{QA16C} = \begin{pmatrix} 3 & -1 \\ 2 & 7 \end{pmatrix} \text{Ag(110)}$$

where the lattice constants of Ag(110) are $a_s = 2.8895$ Å and $b_s = 4.0864$ Å. Therefore, the close-packing model of QA16C on Ag(110) is indicated in Figure 3e. In this model, the alkyl chains of the organic molecules operate as spacers to adjust the intermolecular distance on the saturated QA16C monolayer. The strong intermolecular interactions support the stability of the final rowlike QA16C structure.

When the saturation monolayer is complete, it is interesting to note that the step-edge alignment induced by the adsorbed QA16C molecules is observed. Figure 4a,b shows the straight step edges of the Ag(110) surface in the [5−53] direction up to one hundred nanometers at QA16C monolayer coverage. It should be noticed that only step edges with single-atom height can be modified by the adsorbate, possibly because of the higher diffusion barrier when organic molecules try to affect step edges

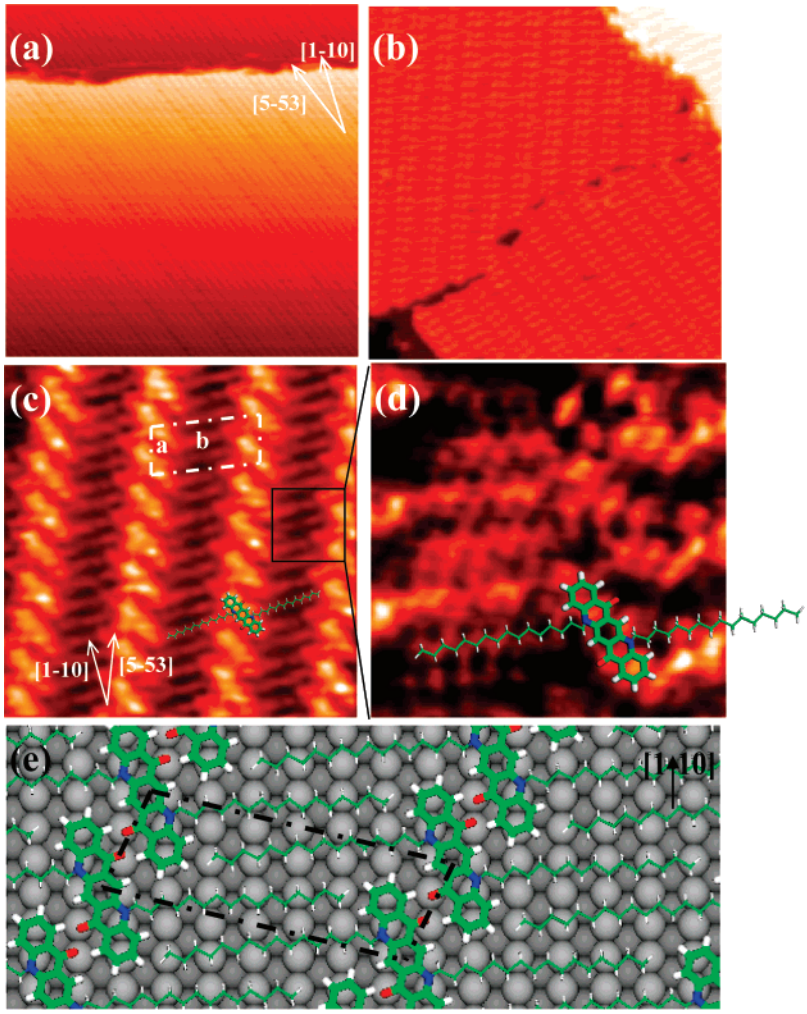

Figure 3. (a) Large-scale STM image of QA16C monolayer deposited on the Ag(110) surface. Conditions: area = 150 nm × 150 nm, V_{sample} = 2.0 V, I = 0.05 nA. (b) Two symmetrical QA16C domains on the same terrace. This boundary is irregular, and some holes can be observed because of the mismatch between these two structures. Conditions: area = 37 nm × 37 nm, V_{sample} = −1.0 V, I = 0.1 nA. (c) High-resolution STM image of QA16C monolayer deposited on the Ag(110) surface. The QA16C molecule is displayed in this image with a ball-and-stick model. The QA16C molecules are organized into rows along the [5−53] direction and are separated by the alkyl chains, which are interdigitated over their full length and aligned with their long axis parallel to the substrate surface. Conditions: area = 10 nm × 10 nm, V_{sample} = 1.0 V, I = 0.21 nA. (d) Details of alkyl chains between QA16C molecules, suggesting that the alkyl chain plane lies parallel to the substrate. Conditions: area = 3.36 nm × 3.36 nm, V_{sample} = −1.5 V, I = 0.6 nA. (e) Proposed model of QA16C on the Ag(110) surface.

with multiatom heights. From the enlarged images of Figure 4c and d, we conclude that the uniform structure of QA16C molecules extends continuously over the neighboring terraces with a height difference of single silver atom and that silver substrate atoms at the step edges are driven to realign. Taking the symmetry of the Ag(110) surface into account, two equivalent domains of QA16C monolayer should exist, and both are indeed observed in our STM measurement.

It is well-known that the interactions between adsorbed molecules and the silver substrate atoms are stronger at step edges than on flat terraces. The silver step-edge alignment induced by adsorbed QA16C molecules is closely related to the intermolecular interactions and the periodic structure.[30,31] Consequently, all of the affected step edges are aligned along the shortest vector of the unit cell of the QA16C monolayer with a rowlike structure in the [5−53] direction. This structure provides the highest density of adsorbed organic molecules to result in the strongest attractive intermolecular interactions mediated by the substrate silver atoms. Although such step edges with a high coordination number are rare on a clean Ag(110) surface, it is believed that the alignment of the step edges of the silver substrate by the adsorbed organic molecules must be energetically favorable for the saturated monolayer coverage.

Comparing the [5−53] step edges induced by the adsorbed QA16C molecules at monolayer coverage (in Figure 4) and the [20 −20 9] step edges where regular molecular alignment is observed at very low coverage (in Figure 1c,d), we find that there is a slight difference in angle of 4°. This coincidence implies that the straight step edges in the [20 −20 9] direction at very low coverage are most likely induced by QA16C molecules in a manner similar to that found in the case of a saturated monolayer.

3.3. Multilayer Regime. With the careful evaporation of additional molecules, by controlling the deposition time and molecule flux, we imaged the second-layer structure on top of the completed QA16C monolayer. STM images revealed that the QA16C molecules of the second layer form a new rowlike structure that is significantly different from the rowlike pattern of the monolayer structure. Figure 5a shows a typical STM image of about 1.3 ML of QA16C deposited on the Ag(110) surface. The lengths of the rows vary from 10 to 30 nm. The distance between two neighboring rows is 1.82 ± 0.02 or 2.83

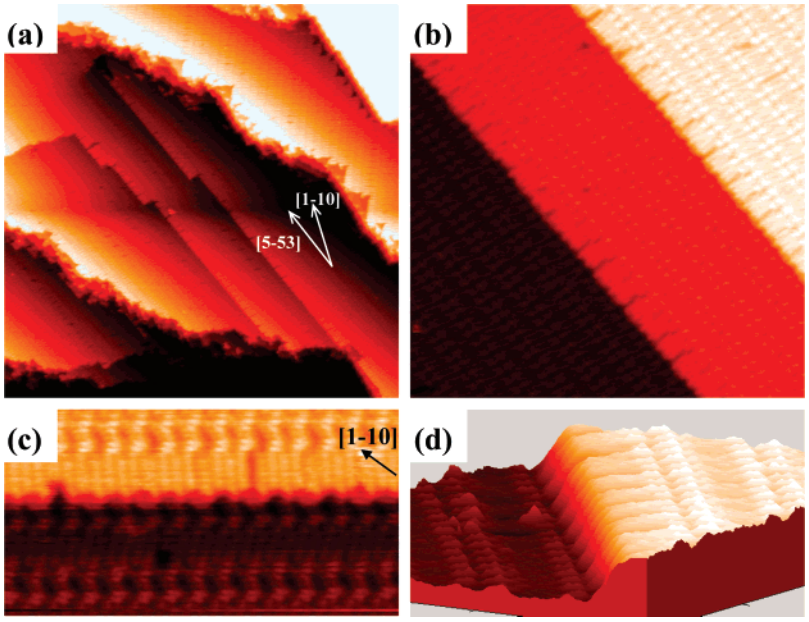

Figure 4. Step-edge alignments induced by the adsorbed QA16C molecules observed when the saturation monolayer is completed. The straight step edges of the Ag(110) surface, along the [5−53] direction, are up to 100 nm at monolayer QA16C coverage. Conditions: (a) area = 135 nm × 135 nm, $V_{sample} = -1.0$ V, $I = 0.15$ nA; (b) area = 36 nm × 36 nm, $V_{sample} = -1.0$ V, $I = 0.1$ nA; (c) area = 16 nm × 8.5 nm, $V_{sample} = -1.0$ V, $I = 2$ nA. This STM image was obtained at a rotation angle of 38°. (d) Three-dimensional image of the induced step edge. Conditions: $V_{sample} = -1.0$ V, $I = 0.08$ nA.

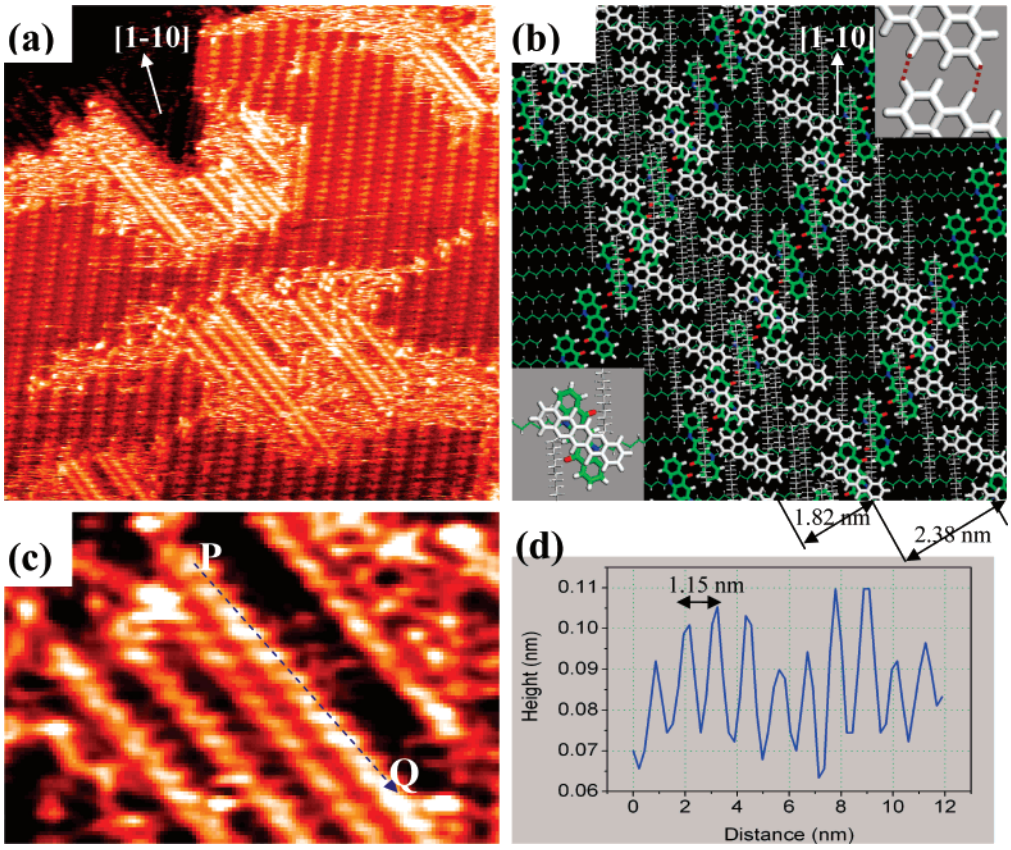

Figure 5. (a) Typical STM image of 1.3 ML of QA16C deposited on Ag(110). The QA16C molecules in the second layer form a rowlike structure. Conditions: area = 80 nm × 80 nm, $V_{sample} = 1.1$ V, $I = 0.03$ nA. (b) Proposed structure. The green and white molecules indicate the first and second layers, respectively. Ag atoms under QA16C are not shown in this sketch. (c) Details of the rowlike QA16C structure in the second layer. Conditions: area = 20 nm × 20 nm, $V_{sample} = 1.1$ V, $I = 0.03$ nA. (d) Line profile across the QA16C row marked by the dashed arrow line from P to Q shown in image c.

± 0.02 nm, or their integer multiples. The angle between the second-layer rows and the Ag[1−10] direction is 23° ± 2°. In the second layer, it is difficult to reveal the details of the interdigitated alkyl chains as spacers between neighboring rows instead of dark regions in STM images, owing to the buffer layer of the first-layer organic molecules. Through the dispersed single molecules in Figure 5a, we can distinguish the adsorption sites of the second-layer QA16C molecules on the first layer.

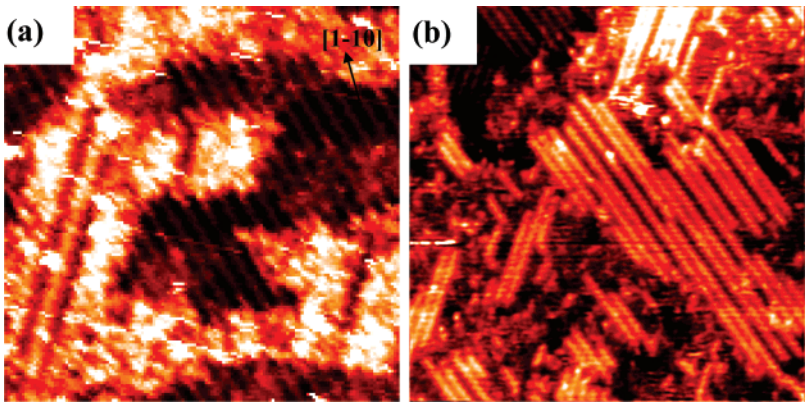

Figure 6. (a) Typical STM image of 1.7 ML of QA16C deposited on Ag(110) at room temperature. Conditions: area = 90 nm × 90 nm, V_{sample} = −1.3 V, I = 0.025 nA. (b) STM image of 1.7 ML of QA16C deposited on Ag(110) when the growth temperature was held at 370 K. The enhanced surface diffusion of QA16C molecules on the substrate helps the formation of rowlike QA16C structures in the second layer. Conditions: area = 60 nm × 60 nm, V_{sample} = 1.1 V, I = 0.03 nA.

The conclusion can be drawn that the backbones of the second-layer QA16C molecules stack on top of those of the first-layer molecules. Therefore, $\pi-\pi$ stacking interactions will enhance the stability of adsorption because the additional molecules stack on the conjugated backbones of the lower QA16C molecules. This situation is quite different from that for the first layer adsorbed directly on the Ag(110) surface. For adsorption of the monolayer, the chemical bonds between the oxygen and silver atoms determine the QA16C adsorption sites on the noble metal substrate. Taking into account the relatively large distance between the substrate and the second layer of organic molecules, the additional QA16C molecules over the first layer should be less affected by the silver substrate.

Figure 5c presents the details of the QA16C rowlike structures. The enlarged view reveals that the flat-lying molecules interact predominantly through their functional groups. The backbones of the QA16C molecules are parallel to each other, make an angle of about 74° ± 2° to the Ag[1−10] direction, and are modulated to keep proper distances. Figure 5d shows the line-scan height profile across a row of QA16C molecules from P to Q, from which we derive 1.15 ± 0.02 nm as the average distance between neighboring molecules in the rows.

Figure 5b shows a schematic drawing of a proposed structure for the QA16C rowlike structures. After completing a saturated monolayer of QA16C, the additional molecules are deposited on the first layer, and their stable adsorption sites are determined by the intermolecular interactions of the $\pi-\pi$ stacking stabilization between the two layers. To avoid overlap between the QA16C molecules in the rows, the backbones of the QA16C molecules in the upper and lower layers are slightly staggered with an angle of about 30°, as shown in the lower left inset of Figure 5b. The interdigitated alkyl chains also appear as spacers to separate the neighboring rows in the same way as they do in the structures of the monolayer. In this model, the distance between the oxygen and hydrogen atoms of neighboring molecules in the rows is 2.35 Å (upper right inset of Figure 5b). Previous studies revealed that a C−H···O bonding interaction occurs when the distance between the oxygen and the hydrogen is within the range of 1.5−3.0 Å.[32,33] Therefore, in the second layer, a type of hydrogen bond with medium intensity is formed between two neighboring molecules of the QA16C rowlike structures. These hydrogen bonds, as attractive intermolecular interactions, play an important role in forming the stable structure of rows in the second layer. In addition to hydrogen bonds, other interactions in the second layer, such as alkyl−alkyl interactions, might also play a role in enhancing the stability of the second-layer structure because interdigitated alkyl chains appear.

It should be specifically pointed out that formation of the second QA16C layer on the Ag(110) substrate is more complex than formation of the QA16C monolayer. In the second-layer structure, only some of the molecules have an opportunity for $\pi-\pi$ stacking with the first layer. As additional QA16C molecules begin to be adsorbed on the first QA16C monolayer, $\pi-\pi$ stacking affects the initial adsorption sites. However, the stability of the structure in the second layer is mostly improved by intrinsic intermolecular interactions, such as hydrogen bonds and alkyl−alkyl interactions. The second layer of organic molecules on a noble metal substrate, because of the larger distance between the molecules and the substrate atoms, should be less affected by molecule−substrate interactions. Consequently, in the second QA16C layer, the hydrogen bonds, alkyl−alkyl interactions, and $\pi-\pi$ interactions play a role in forming a stable structure, which is similar to the reported bulk properties of quinacridone derivatives.[10,34] In 3-dimensional aggregation, $\pi-\pi$ stacking and hydrogen bonds dominate the assembled structure of quinacridone derivatives. It is understandable that the intermolecular interactions could be adjusted for attached different alkyl chains. In this case of QA16C, the interdigitated alkyl chains provide additional contributions to the stability of the molecule assembly on the noble metal surface.

Figure 6a presents a typical STM image of about 1.7 ML of QA16C deposited on the Ag(110) surface at room temperature. At this coverage, rowlike QA16C structures can be observed over the uniform monolayer. However, most of the molecules of the second layer no longer belong to the rowlike structures, but form random clusters with irregular shapes to disperse on the preformed QA16C monolayer. These amorphous structures limit the applications of QA16C in future nanodevices; thus, better growth conditions are needed to improve the quality of the QA16C structure.

Considering that the interactions between QA16C molecules in the second layer play an important role in the construction of a stable rowlike structure, enhancing the surface diffusion of molecules on the substrate will help the formation of rowlike QA16C structures. In this case, more organic molecules should find their suitable positions to assemble uniform structures. Therefore, we increased the growth temperature during the deposition to 370 K and slightly decreased the deposition rate, which can evidently improve the quality of rowlike QA16C structure formation in the second layer. Figure 6b shows a

typical STM image of QA16C nanostructures deposited on the Ag(110) surface at a coverage of about 1.7 ML when the substrate was kept at 370 K during the deposition. In this growth process, the deposited QA16C molecules had a greater ability to diffuse on the surface, especially for those added after 1 ML had been deposited, which had a greater possibility to relax and improve the rowlike structures. Figure 6b shows that many rowlike QA16C structures were formed and that the lengths can reach to 50 nm. Two equivalent orientations of the rows were found because of the different orientations of the QA16C domains in the preformed monolayer when considering the symmetry of the Ag(110) substrate. The rows tend to aggregate with a dimer-row structure. The distance between structures in the dimer row is 1.82 ± 0.02 nm, and the dimer-row distance is 2.38 ± 0.02 nm, which depends on the effect of the stacking site on the QA16C monolayer, as demonstrated in Figure 5b.

4. Conclusions

We studied the overall growth process, from the initial adsorption to the deposition of a second layer, of QA16C molecules deposited on the Ag(110) surface using low-temperature STM. At low coverage, two distinct adsorption sites of single QA16C molecules on the Ag(110) surface are determined by the molecule−substrate interactions. At increasing molecular coverage, the QA16C molecules aggregate into molecular islands on large silver terraces to form a rowlike structure. In the monolayer regime, a close-packed rowlike structure of QA16C molecules is formed and induces the step-edge alignment of the silver substrate. When additional molecules are deposited after the first monolayer, a different rowlike structure appears owing to the lack of strong molecule−substrate interactions.

Acknowledgment. We thank Dr. Zhihai Cheng, Dr. Zhitao Deng, Jichun Lian, Nan Jiang, Qi Liu, and Li Cai for experimental assistance and Prof. Zhiqiang Qiu for manuscript polishing. This work was partially supported by the National Science Foundation of China (NSFC) (Grants 90406022 and 60621061) and National 973 (Grant 2006CB921305) of China.

References and Notes

(1) Service, R. F. *Science* **2005**, *310*, 1762.
(2) Voss, D. *Nature (London)* **2000**, *407*, 442.
(3) Dimitrakopoulos, C. D.; Malenfant, P. R. L. *Adv. Mater.* **2002**, *14*, 99.
(4) Sirringhaus, H.; Tessler, N.; Friend, R. H. *Science* **1998**, *280*, 1741.
(5) Crone, B.; Dodabalapur, A.; Lin, Y. Y.; Filas, R. W.; Bao, Z.; LaDuca, A.; Sarpeshkar, R.; Katz, H. E.; Li, W. *Nature (London)* **2000**, *403*, 521.
(6) Gao, H.-J.; Sohlberg, K.; Xue, Z. Q.; Chen, H. Y.; Hou, S. M.; Ma, L. P.; Fang, X. W.; Pang, S. J.; Pennycook, S. J. *Phys. Rev. Lett.* **2000**, *84*, 1780. Ma, L. P.; Song, Y. L.; Gao, H.-J.; Zhao, W. B.; Chen, H. Y.; Xue, Z. Q.; Pang, S. J. *Appl. Phys. Lett.* **1996**, *69*, 3752. Gao, H.-J.; Xue, Z. Q.; Wang, K. Z.; Wu, Q. D.; Pang, S. *Appl. Phys. Lett.* **1996**, *68*, 2192.
(7) Barth, J. V.; Costantini, G.; Kern, K. *Nature (London)* **2005**, *437*, 671.
(8) Hiramoto, M.; Kawase, S.; Yokoyama, M. *Jpn. J. Appl. Phys.* **1996**, *35*, L349.
(9) Shichiri, T.; Suezaki, M.; Inoue, T. *Chem. Lett.* **1992**, *21*, 1717.
(10) Ye, K.; Wang, J.; Sun, H.; Liu, Y.; Mu, Z.; Li, F.; Jiang, S.; Zhang, J.; Zhang, H.; Wang, Y.; Che, C. *J. Phys. Chem. B* **2005**, *109*, 8008.
(11) Wang, J.; Zhao, Y.; Zhang, J.; Zhang, J.; Yang, B.; Wang, Y.; Zhang, D.; You, H.; Ma, D. *J. Phys. Chem. C* **2007**, *111*, 9177.
(12) Shi, J.; Tang, C. W. *Appl. Phys. Lett.* **1997**, *70*, 1665.
(13) Jabbour, G. E.; Yawabe, Y.; Shaheen, S. E.; Wang, J. F.; Morrell, M. M.; Kippelen, B.; Peyghambarian, N. *Appl. Phys. Lett.* **1997**, *71*, 1762.
(14) Gross, E. M.; Anderson, J. D.; Slaterbeck, A. F.; Thayumanavan, S.; Barlow, S.; Zhang, Y.; Marder, S. R.; Hall, H. K.; Nabor, M. F.; Wang, J.-F.; Mash, E. A.; Armstrong, N. R.; Wightman, R. M. *J. Am. Chem. Soc.* **2000**, *122*, 4972.
(15) Keller, U.; Mullen, K.; De Feyter, S.; De Schryver, F. C. *Adv. Mater.* **1996**, *8*, 490.
(16) De Feyter, S.; Gesquiere, A.; De Schryver, F. C.; Keller, U.; Mullen, K. *Chem. Mater.* **2002**, *14*, 989.
(17) Yang, X.; Wang, J.; Zhang, X.; Wang, Z.; Wang, Y. *Langmuir* **2007**, *23*, 1287.
(18) Mu, Z.; Wang, Z.; Zhang, X.; Ye, K.; Wang, Y. *J. Phys. Chem. B* **2004**, *108*, 19955.
(19) Yang, X.; Mu, Z.; Wang, Z.; Zhang, X.; Wang, J.; Wang, Y. *Langmuir* **2005**, *21*, 7225.
(20) Cheng, Z. H.; Gao, L.; Deng, Z. T.; Liu, Q.; Jiang, N.; Lin, X.; He, X. B.; Du, S. X.; Gao, H.-J. *J. Phys. Chem. C* **2007**, *111*, 2656.
(21) Lin, F.; Zhong, D. Y.; Chi, L. F.; Ye, K.; Wang, Y.; Fuchs, H. *Phys. Rev. B* **2006**, *73*, 235420.
(22) Shi, D. X.; Ji, W.; Lin, X.; He, X. B.; Lian, J. C.; Gao, L.; Cai, J. M.; Lin, H.; Du, S. X.; Lin, F.; Seidel, C.; Chi, L. F.; Hofer, W. A.; Fuchs, H.; Gao, H.-J. *Phys. Rev. Lett.* **2006**, *96*, 226101.
(23) Muller, T.; Werblowsky, T. L.; Florio, G. M.; Berne, B. J.; Flynn, G. W. *Proc. Natl. Acad. Sci. U.S.A.* **2005**, *102*, 5315.
(24) Gao, L.; Deng, Z. T.; Ji, W.; Lin, X.; Cheng, Z. H.; He, X. B.; Shi, D. X.; Gao, H.-J. *Phys. Rev. B* **2006**, *73*, 075424.
(25) Pan, G.; Cheng, X.; Hoger, S.; Freyland, W. *J. Am. Chem. Soc.* **2006**, *128*, 4218. Qiu, X. H.; Wang, C.; Zeng, Q. D.; Xu, B.; Yin, S. X.; Wang, H. N.; Xu, S. D.; Bai, C. L. *J. Am. Chem. Soc.* **2000**, *122*, 5550. De Feyter, S.; De Schryver, F. C. *Chem. Soc. Rev.* **2003**, *32*, 139.
(26) Wei, Y.; Kannappan, K.; Flynn, G. W.; Zimmt, M. B. *J. Am. Chem. Soc.* **2004**, *126*, 5318.
(27) De Feyter, S.; De Schryver, F. C. *J. Phys. Chem. B* **2005**, *109*, 4290.
(28) Mamdouh, W.; Uji-i, H.; Ladislaw, J. S.; Dulcey, A. E.; Percec, V.; De Schryver, F. C.; De Feyter, S. *J. Am. Chem. Soc.* **2006**, *128*, 317.
(29) Cyr, D. M.; Venkataraman, B.; Flynn, G. W. *Chem. Mater.* **1996**, *8*, 1600.
(30) Chen, Q.; Richardson, N. V. *Prog. Surf. Sci.* **2003**, *73*, 59.
(31) Jeong, H.-C.; Williams, E. D. *Surf. Sci. Rep.* **1999**, *34*, 171.
(32) Jeffrey, G. A. *J. Mol. Struct.* **1999**, *485*−*486*, 293.
(33) Barth, J. V.; Weckesser, J.; Cai, C.; Gunter, P.; Burgi, L.; Jeandupeux, O.; Kern, K. *Angew. Chem., Int. Ed.* **2000**, *39*, 1230.
(34) Sun, H.; Ye, K.; Wang, C.; Qi, H.; Li, F.; Wang, Y. *J. Phys. Chem. A* **2006**, *110*, 10750.